

Cite this article as: Neural Regen Res. 2012;7(16):1213-1219.

# Morphological properties and proliferation analysis of olfactory ensheathing cells seeded onto three-dimensional collagen-heparan sulfate biological scaffolds<sup>☆</sup>

Na Liu, Zhouping Tang, Zhiyuan Yu, Minjie Xie, Yu Zhang, Erfang Yang, Shabei Xu

Department of Neurology, Tongji Hospital, Tongji Medical College, Huazhong University of Science and Technology, Wuhan 430030, Hubei Province, China

## Abstract

This study aimed to examine the differences in the morphological properties and proliferation of olfactory ensheathing cells in three-dimensional culture on collagen-heparan sulfate biological scaffolds and in two-dimensional culture on common flat culture plates. The proliferation rate of olfactory ensheathing cells in three-dimensional culture was higher than that in two-dimensional culture, as detected by an MTT assay. In addition, more than half of the olfactory ensheathing cells subcultured using the trypsinization method in three-dimensional culture displayed a spindly Schwann cell-like morphology with extremely long processes, while they showed a flat astrocyte-like morphology in two-dimensional culture. Moreover, spindle-shaped olfactory ensheathing cells tended to adopt an elongated bipolar morphology under both culture conditions. Experimental findings indicate that the morphological properties and proliferation of olfactory ensheathing cells in three-dimensional culture on collagen-heparan sulfate biological scaffolds are better than those in two-dimensional culture.

## Key Words

morphological properties; cell proliferation; biological scaffold; olfactory ensheathing cells; three-dimensional culture; neural regeneration

## Abbreviations

OECs, olfactory ensheathing cells; p75 NGFR, p75 nerve growth factor receptor; GFAP, glial fibrillary acid protein; CFSE, carboxyfluorescein diacetate succinimidyl ester

Na Liu<sup>☆</sup>, Studying for doctorate, Department of Neurology, Tongji Hospital, Tongji Medical College, Huazhong University of Science and Technology, Wuhan 430030, Hubei Province, China

Na Liu and Zhouping Tang contributed equally to this work.

Corresponding author: Shabei Xu, M.D., Professor, Department of Neurology, Tongji Hospital, Tongji Medical College, Huazhong University of Science and Technology, Wuhan 430030, Hubei Province, China ddjtzp@163.com

Received: 2012-01-15

Accepted: 2012-04-23  
(N20120115001/WJ)

Liu N, Tang ZP, Yu ZY, Xie MJ, Zhang Y, Yang EF, Xu SB. Morphological properties and proliferation analysis of olfactory ensheathing cells seeded onto three-dimensional collagen-heparan sulfate biological scaffolds. Neural Regen Res. 2012;7(16):1213-1219.

www.crter.cn  
www.nrronline.org

doi:10.3969/j.issn.1673-5374.2012.16.002

## INTRODUCTION

Olfactory ensheathing cells (OECs) are a promising and popular strategy for spinal cord injury therapy, and can support neurogenesis throughout life in the olfactory system<sup>[1]</sup>. They are the resident glial cells of the primary olfactory nerve and share some common features with Schwann cells and astrocytes<sup>[2]</sup>. These cells cannot only extend processes to enwrap the axons of the primary olfactory neurons, but also form a

permissive cellular pathway for growing axons of new adult-born primary olfactory neurons. OECs appear to promote a wide range of processes that are beneficial for spinal cord repair after transplantation in the spinal cord<sup>[3-4]</sup>. OECs also have been reported to myelinate axons<sup>[5-6]</sup> and promote the survival of injured neurons and partial functional recovery after transplantation<sup>[7-8]</sup>. Furthermore, OECs can adapt quickly to foreign cellular environments where they may play a positive role in wound healing and regenerative response<sup>[9]</sup>. The positive

reaction is shown by their diverse morphology. Usually, OECs exhibit different morphologies *in vitro*, related to the age and source of the tissue donor, the method of isolation, and the culture conditions<sup>[10-11]</sup>. OECs have been cultured from the olfactory epithelium, lamina propria, olfactory nerves, and the outer olfactory bulb layer of embryonic, neonatal or adult rats and mice. In two-dimensional (2-D) culture conditions, OECs display a range of distinct morphologies: flat, spindle, and stellate. Moreover, many studies have demonstrated that cultured OECs can spontaneously transform from one morphological type to another<sup>[12-13]</sup>. The morphology of OECs is also affected by extracellular and intracellular molecules such as cyclic adenosine monophosphate (cAMP), endothelin-1 and fibulin-3<sup>[12, 14-15]</sup>. However, little is known about the morphological properties of OECs in three-dimensional (3-D) culture. With the development of biological scaffolds, it is necessary to study the morphological properties of OECs in 3-D culture environment, because these data can help to evaluate the viability and motility of OECs before guidelines can be developed for the transplantation of OECs with biological scaffolds.

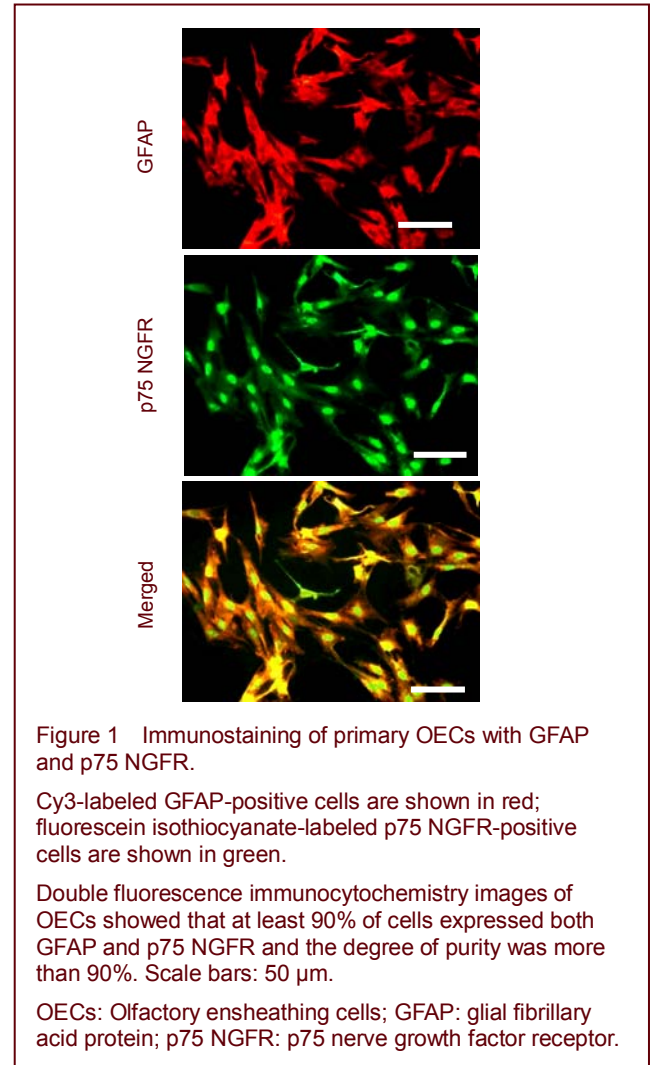
Based on the above background, the aim of this study was to reveal the differences in the morphological properties and proliferation of OECs in 3-D culture and 2-D culture environment. In 3-D culture environment, we used 3-D collagen-heparan sulfate (CHS) biological scaffolds. This study analyzed the percentages of morphological types, process length, process number, growth and proliferation of OECs in both 2-D and 3-D culture environment. This study allows us to better understand the morphological properties and proliferation of OECs in 3-D culture environment, which may be influential factors for the effectiveness of transplantation.

## RESULTS

### Primary culture and purification of neonatal rat OECs

In this study, primary cultures of OECs were derived by combining the basic method and the cytarabine method. By 7–10 days, primary cultures had usually reached a confluence under phase-contrast microscopy. As usual, OECs growing in the serum-containing medium mainly appeared to adopt spindle, flat and stellate morphologies. They were identified in culture by their characteristic morphology and the expression of p75 nerve growth factor receptor (p75 NGFR) and glial fibrillary acid protein (GFAP). To examine the purity of primary OECs, they were stained for p75 NGFR and GFAP for fluorescence immunocytochemical analysis. Double fluorescence immunocytochemical analysis of OECs showed that at

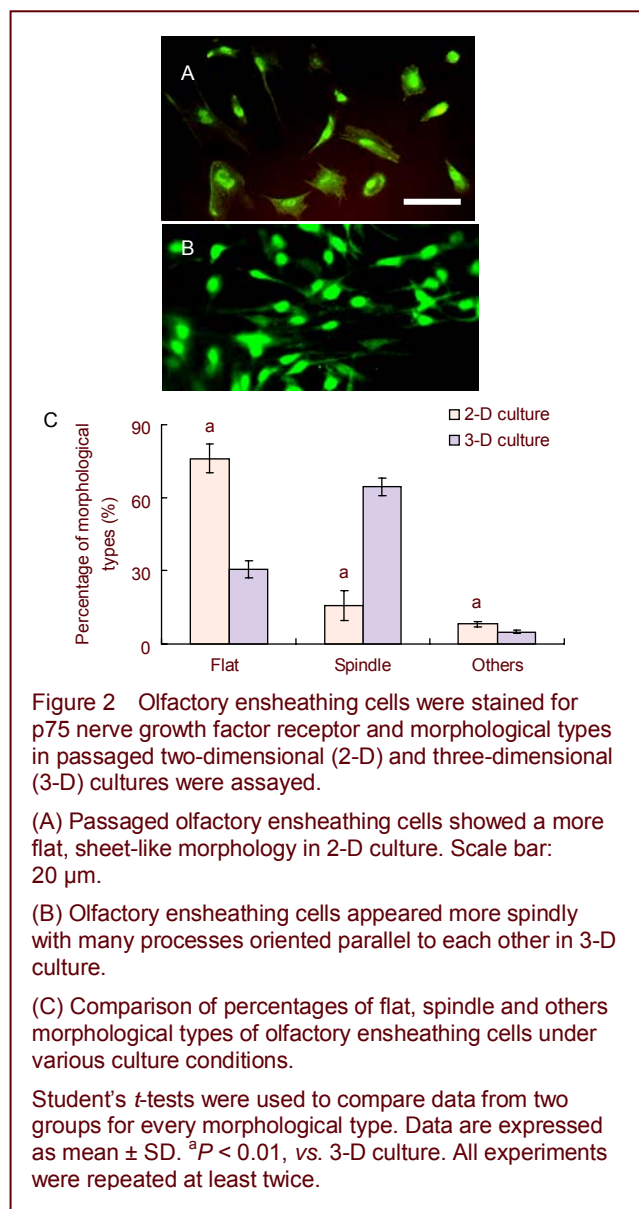
least 90% of cells co-expressed p75 NGFR and GFAP (Figure 1). In other words, the degree of purity was more than 90%. Moreover, it suggested that these cells were suitable to use for further experiments.



### Assay for OEC morphological properties

In this study, OECs exhibited very distinct morphological features in 3-D culture environment on CHS scaffolds and 2-D culture environment on common flat culture plates, as shown by immunostaining with p75 NGFR. In primary 3-D culture environment, most OECs were spindle-shaped. In contrast, during many passages of OECs by trypsinization, the cells showed a flat, astrocyte-like morphology in 2-D culture environment. As shown in Figures 2A and 3C, passaged OECs in 2-D culture environment mostly showed a flat, sheet-like shape for 4 days. Otherwise, OECs passaged by trypsinization in 3-D CHS scaffolds maintained the primary culture spindle morphology with long processes, like Schwann cells (Figures 2B and 3D). The cell body in 3-D culture environment was bigger than that in 2-D culture environment at the same magnification (Figures 2A, B and 3C, D). By statistical analysis, the percentage

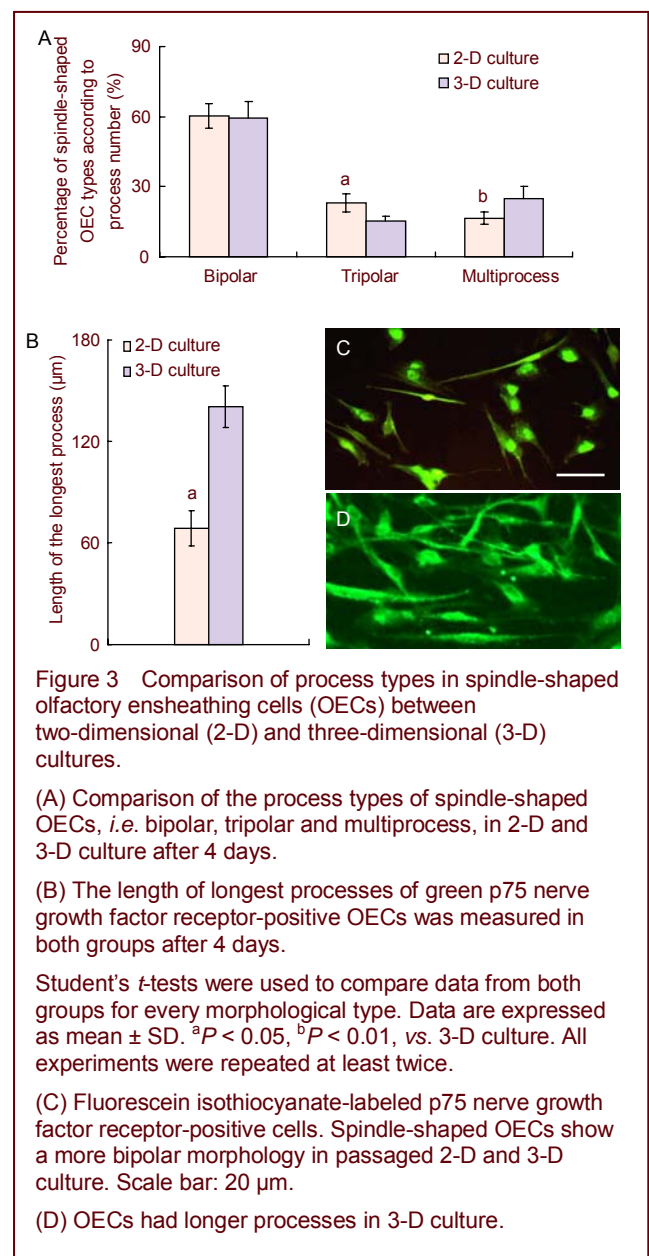
of spindle OECs in 3-D culture was higher than that in 2-D culture environment for 4 days (Figure 2C). The percentage of flat OEC morphological types was significantly lower in 3-D environment than that in 2-D culture environment for 4 days ( $P < 0.01$ ; Figure 2C). But the percentage of the bipolar type of cells, according to process number per cell, showed no significant difference between the spindle-shaped OECs between two groups ( $P > 0.05$ ; Figure 3A). Moreover, the differences in the percentages of tripolar and multiprocess cell types were significant between the two groups for the spindle-shaped OECs ( $P < 0.05$ ; Figure 3A). In addition, the longest processes of the OECs in 3-D CHS biological scaffolds were significantly longer than those in 2-D culture environment after 4 days ( $P < 0.01$ ; Figure 3B).

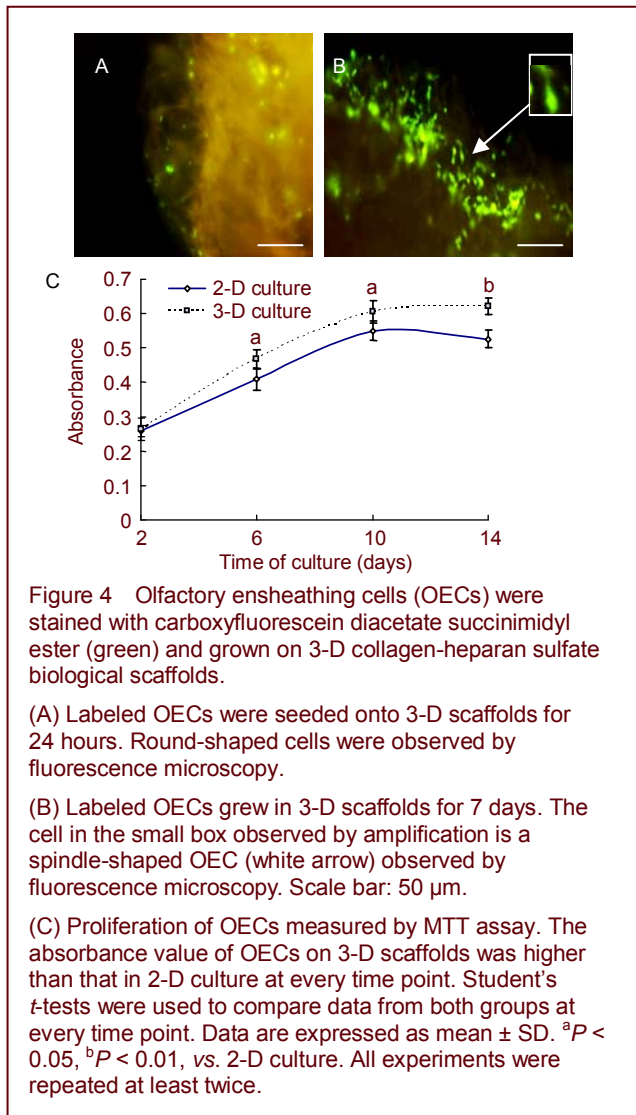


### Assay for OEC proliferation

In this study, OECs always maintained a good viability, especially in 3-D culture. Absorbance values detected by

an MTT assay were different at days 2, 6, 10 and 14 in passaged 2-D and 3-D culture. Figure 4C shows that the absorbance values of OECs on 3-D CHS biological scaffolds were higher than those in 2-D culture after 2, 6, 10 and 14 days. The differences in the absorbance values between cells cultured in 3-D and 2-D culture were significant after 6, 10, and 14 days ( $P < 0.05$ ). Thus, OECs had a higher proliferation rate in 3-D culture. However, there was no significant difference between the two groups after 2 days ( $P > 0.05$ ). By carboxyfluorescein diacetate succinimidyl ester (CFSE) staining, OECs were observed and traced directly under fluorescent microscopy in 3-D culture (Figures 4A, B). Figures 4A, B showed that OECs adhered to scaffolds with a round shape for 24 hours and proliferated in scaffolds for 7 days. Spindle-shaped OECs were also observed for 7 days (Figure 4B).

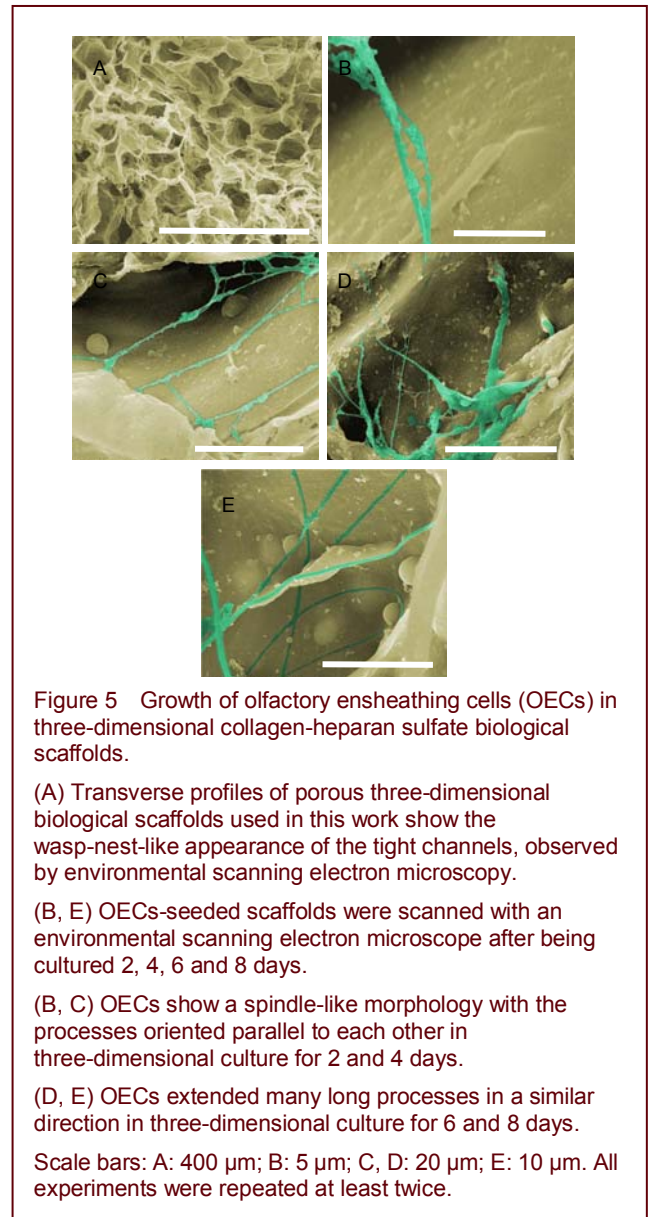




### Growth of the OECs in 3-D CHS biological scaffolds observed by environmental scanning electron microscopy

Transverse sections of 3-D CHS biological scaffolds showed a high degree of porosity by environmental scanning electron microscopy, similar to a wasp nest or sponge (Figure 5A). There were many straight and tightly packed channels in the scaffold. Most of the channels were 50 to 70  $\mu$ m in diameter. Environmental scanning electron microscopy images showed that OECs adhered and grew in scaffolds for 2, 4, 6 and 8 days (Figures 5B–E). OECs mostly appeared with a Schwann cell-like morphology, with two processes and a long fusiform bipolar shape (Figures 5B–D). Moreover, their fine long processes oriented parallel to each other, attached to and crawled along the walls of the scaffold, and extended toward the same direction in 3-D culture (Figures 5B–D). Others were suspended within the lumen and branched at the walls of the scaffold, like vines. Furthermore, the morphological properties of OECs observed by environmental scanning electron

microscopy corresponded to the fluorescence immunocytochemical analysis.



## DISCUSSION

To examine the morphological properties and proliferation of OECs in 3-D culture, we used 3-D CHS biological scaffolds. The scaffolds took on the optimum 3-D structure, like a wasp-nest or sponge, with a relatively uniform aperture, a high degree of porosity and many longitudinal oriented microtubules. Moreover, they had excellent biocompatibility with OECs<sup>[16]</sup>. OECs easily attached to them without pre-coating. They promoted the attachment, viability and proliferation of OECs. Compared with 2-D culture, 3-D CHS scaffold culture promoted better proliferation of OECs. The increased proliferation of OECs in 3-D culture may be due to the optimum 3-D structure and unique components of CHS



scaffolds, because optimum 3-D structure offers enough solid spaces for cell growth and played a guiding role in cell migration. OECs in 3-D culture may receive more signals from each other to promote cell division and growth. The unique components of CHS also contribute to the growth and adhesion of OECs. CHS biological scaffold materials are derived from the extracellular matrix. Collagen can stay stable for a long time and promote attachment, proliferation and aligned process extension of cells<sup>[17]</sup>. Heparan sulfate can interact with the heparin-binding domains of growth and adhesive proteins so that the biochemical characteristics and biological activity of these proteins are altered. These advantages provide a foundation for promoting cell adhesion, growth and proliferation<sup>[18]</sup>.

In this study, the morphological properties of OECs were affected in 3-D culture. After identification with antibodies against two common OEC marker proteins (GFAP and p75 NGFR), the purified OECs were seeded onto scaffolds and poly-L-lysine coated coverslips. 3-D CHS scaffold culture resulted in a significantly greater proportion of spindly Schwann cell-like passaged OECs with extremely long processes. On the contrary, in 2-D culture, the majority of passaged OECs, grown in the same medium as the 3-D cultures, exhibited a flat astrocyte-like morphology. Moreover, the longest processes of the OECs in 3-D scaffolds were significantly longer than those in 2-D culture. The OECs in 3-D culture also was bigger than that in 2-D culture. However, most of spindle-shaped OECs displayed a bipolar type with two long and fine processes in both 2-D and 3-D culture. Thus, OECs exhibited an intrinsic plasticity in morphology, independent of environmental stimuli. Unlike neurons and astrocytes, which have relatively stable morphologies, OECs display highly variable morphology. Interestingly, spindle-shaped OECs preferred to adopt a more elongated bipolar morphology under different culture conditions. This bipolar morphology may allow OECs to obtain more signals from each other to promote cell proliferation. Furthermore, spindle-shaped Schwann cell-like OECs, but not astrocyte-like OECs, have been considered to be a regeneration-promoting phenotype since they myelinate axons and promote neurite outgrowth more effectively<sup>[19]</sup>. This property of spindle-shaped OECs may be due in part to their higher motility<sup>[12]</sup>. OECs always facilitate the growth of axons across the glial scar successfully, adopting a spindle-shaped morphology like Schwann cells<sup>[20]</sup>. Thus, it is crucial to selectively transplant Schwann cell-like OECs for improving the therapeutic properties of OECs in treating spinal cord injury. In summary, the results of this study demonstrated that 3-D scaffold culture, compared with 2-D culture, promoted OEC adhesion, growth, proliferation,

morphological plasticity and process extension. Moreover, 3-D CHS biological scaffolds seeded with OECs may be a better approach for spinal cord injury treatment. Due to the morphological complexity and functional diversity of OECs, further studies are necessary to characterize the specific gene expression profile of OECs, identify factors that influence the therapeutic efficacy of OECs, as well as to develop methods for generating clinically applicable volumes of well-characterized OECs. These will be helpful in achieving successful therapeutic exploration.

## MATERIALS AND METHODS

### Design

A cell culture study involving tissue engineering *in vitro*.

### Time and setting

Experiments were performed at the Laboratory of the Department of Neurology, Tongji Hospital, Tongji Medical College, Huazhong University of Science and Technology, China from September 2009 to October 2010.

### Materials

Twenty neonatal Sprague-Dawley rats within 24 hours of birth, were provided by the Experimental Animal Center, Tongji Medical College, Huazhong University of Science and Technology, China (License No. SCXK (E) 2010-0009). The animal procedures were strictly performed in accordance with the *Guidance Suggestions for the Care and Use of Laboratory Animals*, issued by the Ministry of Science and Technology of China<sup>[21]</sup>. Efforts were made to lessen the number of animals used and their suffering in our study. We prepared the 3-D CHS biological scaffolds ourselves. OECs were obtained from the olfactory bulbs of 3-day old Wistar rats.

### Methods

#### Cell culture

Primary neonatal rat OECs were isolated and cultured as previously described<sup>[16]</sup>. Ten 3-day-old Wistar rats were sacrificed to obtain the olfactory bulbs. OECs isolated from the external olfactory nerve layers were cultured at a final density of  $5 \times 10^4$  cells/mL in flasks coated with 10 µg/mL poly-L-lysine. The culture was fed with fresh DMEM/F12 supplemented with 10% fetal bovine serum (Hyclone, Logan, UT, USA), forskolin (20 M; Sigma, St. Louis, MO, USA), bovine pituitary extract (20 µg/mL; Sigma), penicillin (100 U/mL; Sigma) and streptomycin (100 U/mL; Sigma). To obtain more homogenous OECs, the culture was treated after 24 hours with  $10^{-5}$  M cytosine arabinoside for 2 days and the medium was

refreshed. After 8–10 days, the primary cultures were passaged. Finally, OECs were harvested once a week for 2–3 weeks for use<sup>[22]</sup>. To further study the morphology properties of OECs, 1 mL of purified OEC suspension was used to seed the cells into 3-D CHS biological scaffolds (3-D culture experimental groups), or poly-L-lysine-coated coverslips (2-D culture control groups) in 24-well plates, at a density of  $3 \times 10^5$  cells/mL. Moreover, the medium was refreshed every 3 days.

### **3-D CHS biological scaffold preparation**

3-D CHS biological scaffolds were prepared as previously described<sup>[16]</sup>. Heparan sulfate (Sigma), type I (Sigma) and type IV (Abcam, Cambridge, UK) collagens, were dissolved to final concentrations of 10, 1.5 and 0.1 mg/mL respectively in a solution of 0.05 M sterile acetic acid (pH 3–4) and mixed at 4°C, 5 000 r/min in a blender (78HW-I, Jiangsu Jintan Co., China). The suspension was then degassed under vacuum (50 mTorr) at room temperature for 60 minutes and was stored at 4°C. It was degassed again right before use and injected into a silica gel pipe (10 cm length, 3 mm diameter) at –80°C for 2 hours. The pipe was cut into cylindrical columns (2 cm length, 3 mm diameter) and immediately placed into the chamber of a freeze-dryer (FD-1-50, Beijing Boyikang Co., China) under vacuum (100 mTorr) at –30°C for 24 hours to prepare 3-D CHS scaffolds with parallel oriented pores<sup>[23]</sup>. After exposure to ultraviolet rays (500 mW/m<sup>2</sup>) for 2 hours, the cross-linked and sterile desiccated scaffolds were put into storage at 4°C.

### **Fluorescence immunocytochemical and CFSE staining**

Immunocytochemistry procedures were performed as described previously by Ramon-Cueto and Valverde<sup>[24]</sup>. In brief, OECs were fixed with 4% paraformaldehyde at 37°C for 15 minutes. After being washed three times with PBS, the cells were permeabilized with 0.05% Triton X-100 in PBS for 15 minutes and immuno-blocked with 1% (w/v) fetal bovine serum in PBS for 60 minutes. To test the purity of OECs, they were incubated with polyclonal rabbit anti-p75 NGFR antibody (1:200; Sigma) and mouse monoclonal anti-GFAP (1:200; Santa Cruz Biotechnology, Santa Cruz, CA, USA). Then samples were incubated with FITC-labeled goat anti-rabbit IgG antibody (1:100; Sigma) and Cy3-labeled rabbit anti-mouse antibody (1:100; Sigma)<sup>[25]</sup>. Parallel negative controls were subjected to the same procedures by incubating cells with only the secondary antibodies. In addition, suspensions of purified OECs were centrifuged at 1 000 r/min for 10 minutes and resuspended in PBS for CFSE staining. Then, 5 mM CFSE (Sigma) was diluted to 2 mM in PBS. OECs labeled by CFSE can be observed and traced directly under the fluorescent

microscopy in 3-D culture. All samples were scanned under a fluorescence microscope (Olympus, Tokyo, Japan) and the images were analyzed with the ImageJ program (National Institutes of Health, USA).

### **OEC proliferation measured by MTT assay**

The proliferation rate of OECs was measured using MTT (Sigma) assay in 2-D and 3-D culture. The cells not labeled with CFSE ( $1 \times 10^4$  cells/200  $\mu$ L) were plated onto 3-D CHS biological scaffolds (3-D culture experimental groups), or poly-L-lysine-coated coverslips (2-D culture control groups) in 96-well plates and incubated at 37°C and 5% CO<sub>2</sub> for 2, 6, 10, and 14 days. After the wells were washed once with PBS, MTT solution was added to each well at a final concentration equal to 10% of the medium. After incubation for 4 hours at 37°C, the supernatant was removed and 150  $\mu$ L dimethylsulfoxide (Sigma) was added into each well. Then 96-well plates were placed on a microtiter plate shaker for 15 minutes. The absorbance of the cell lysates was detected at 570 nm by a microplate reader (Multiskan MK3, Thermo Labsystems, Finland). The reference wave length was at 630 nm<sup>[26-27]</sup>. All absorbance values present in this study are the original absorbance values in 2-D and 3-D groups minus the mean of absorbance values in 2-D and 3-D control groups, to avoid interference from the scaffold and culture medium.

### **Environmental scanning electron microscope**

At days 2, 4, 6 and 8, seeded scaffolds for environmental scanning electron microscopy were fixed with 4% glutaraldehyde for 4 hours and dehydrated in acetone using a critical point dryer. Non-seeded and seeded samples were mounted on stubs and sputter-coated with gold. They were then loaded into an environmental scanning electron microscope (Quanta 200, FEI Co., Eindhoven, Netherlands) and scanned<sup>[28]</sup>.

### **Statistical analysis**

We measured and calculated the lengths of the longest processes, process number and morphological types of OECs from 40 random non-overlapping fields in 2-D and 3-D culture. All data obtained from assays were analyzed, averaged, and expressed as mean  $\pm$  SD and Student's *t*-tests were used to compare data from different groups. Statistical analysis was evaluated by SPSS 12.0 software (SPSS, Chicago, IL, USA). Significance was accepted at  $P < 0.05$ .

**Funding:** This study was financially sponsored by the National Natural Science Foundation of China, No. 30570628, 30770751 and 81171089.

**Author contributions:** Na Liu, Zhouping Tang and Shabei Xu

designed this study. Na Liu wrote this article. Na Liu, Yu Zhang and ErfangYang performed the experiments and collected data. Na Liu and Zhouping Tang analyzed all data in this study. Zhiyuan Yu and Minjie Xie provided experimental technical and data support.

**Conflicts of interest:** None declared.

**Ethical approval:** The experiments were approved by the Animal Ethics Committee, Tongji Hospital, Tongji Medical College, Huazhong University of Science and Technology, China.

## REFERENCES

- [1] Raisman G, Li Y. Repair of neural pathways by olfactory ensheathing cells. *Nat Rev Neurosci*. 2007;8(4):312-319.
- [2] Devon R, Doucette R. Olfactory ensheathing cells myelinate dorsal root ganglion neurite. *Brain Res*. 1992;589(1):175-179.
- [3] Wewetzer K, Radtke C, Kocsis J, et al. Species-specific control of cellular proliferation and the impact of large animal models for the use of olfactory ensheathing cells and Schwann cells in spinal cord repair. *Exp Neurol*. 2011;299(1):80-87.
- [4] Lindsay SL, Riddell JS, Barnett SC. Olfactory mucosa for transplant-mediated repair: a complex tissue for a complex injury? *Glia*. 2010;58(2):125-134.
- [5] Dombrowski MA, Sasaki M, Lankford KL, et al. Myelination and nodal formation of regenerated peripheral nerve fibers following transplantation of acutely prepared olfactory ensheathing cells. *Brain Res*. 2006;1125(1):1-8.
- [6] Franklin RJ, Gilson JM, Franceschini IA, et al. Schwann cell-like myelination following transplantation of an olfactory bulb-ensheathing cell line into areas of demyelination in the adult CNS. *Glia*. 1996;17(3):217-224.
- [7] Ramón-Cueto A, Plant GW, Avila J, et al. Long-distance axonal regeneration in the transected adult rat spinal cord is promoted by olfactory ensheathing glia transplants. *J Neurosci*. 1998;18(10):3803-3815.
- [8] Toft A, Scott DT, Barnett SC, et al. Electrophysiological evidence that olfactory cell transplants improve function after spinal cord injury. *Brain*. 2007;130(Pt 4):970-984.
- [9] Plant GW, Harvey AR, Leaver SG, et al. Olfactory ensheathing glia: repairing injury to the mammalian visual system. *Exp Neurol*. 2011;229(1):99-108.
- [10] Ramón-Cueto A, Avila J. Olfactory ensheathing glia: properties and function. *Brain Res Bull*. 1998;46(3):175-187.
- [11] Su Z, He C. Olfactory ensheathing cells: biology in neural development and regeneration. *Prog Neurobiol*. 2010;92(4):517-532.
- [12] Huang ZH, Wang Y, Cao L, et al. Migratory properties of cultured olfactory ensheathing cells by single-cell migration assay. *Cell Res*. 2008;18(4):479-490.
- [13] Radtke C, Lankford KL, Wewetzer K, et al. Impaired spinal cord remyelination by long-term cultured adult porcine olfactory ensheathing cells correlates with altered in vitro phenotypic properties. *Xenotransplantation*. 2010;17(1):71-80.
- [14] Vukovic J, Ruitenberg MJ, Roet K, et al. The glycoprotein fibulin-3 regulates morphology and motility of olfactory ensheathing cells in vitro. *Glia*. 2009;57(4):424-443.
- [15] Vincent AJ, West AK, Chuah MI. Morphological plasticity of olfactory ensheathing cells is regulated by Camp and endothelin-1. *Glia*. 2003;41(4):393-403.
- [16] Tang ZP, Liu N, Li ZW, et al. In vitro evaluation of the compatibility of a novel collagen-heparan sulfate biological scaffold with olfactory ensheathing cells. *Chin Med J (Engl)*. 2010;123(10):1299-1304.
- [17] Itoh S, Takakuda K, Kawabata S, et al. Evaluation of cross-linking procedures of collagen tubes used in peripheral nerve repair. *Biomaterials*. 2002;23(23):4475-4481.
- [18] Zisch AH, Zeisberger SM, Ehrbar M, et al. Engineered fibrin matrices for functional display of cell membrane-bound growth factor-like activities: study of angiogenic signaling by ephrin-B2. *Biomaterials*. 2004;25(16):3245-3257.
- [19] Kumar R, Hayat S, Felts P, et al. Functional differences and interactions between phenotypic subpopulations of olfactory ensheathing cells in promoting CNS axonal regeneration. *Glia*. 2005;50(1):12-20.
- [20] Li Y, Field PM, Raisman G. Regeneration of adult rat corticospinal axons induced by transplanted olfactory ensheathing cells. *J Neurosci*. 1998;18(24):10514-10524.
- [21] The Ministry of Science and Technology of the People's Republic of China. Guidance Suggestions for the Care and Use of Laboratory Animals. 2006-09-30.
- [22] Chung RS, Woodhouse A, Fung S, et al. Olfactory ensheathing cells promote neurite sprouting of injured axons in vitro by direct cellular contact and secretion of soluble factors. *Cell Mol Life Sci*. 2004;61(10):1238-1245.
- [23] O'Brien FJ, Harley BA, Yannas IV, et al. The effect of pore size on cell adhesion in collagen-GAG scaffolds. *Biomaterials*. 2005;26(4):433-441.
- [24] Ramon-Cueto A, Valverde F. Olfactory bulb ensheathing glia: a unique cell type with axonal growth-promoting properties. *Glia*. 1995;14(3):163-173.
- [25] Miedzybrodzki R, Tabakow P, Fortuna W, et al. The olfactory bulb and olfactory mucosa obtained from human cadaver donors as a source of olfactory ensheathing cells. *Glia*. 2006;54(6):557-565.
- [26] Feng L, Meng H, Wu F, et al. Olfactory ensheathing cells conditioned medium prevented apoptosis induced by 6-OHDA in PC12 cells through modulation of intrinsic apoptotic pathways. *Int J Dev Neurosci*. 2008;26(3-4):323-329.
- [27] Li J, Chen Y, Mak AF, et al. A one-step method to fabricate PLLA scaffolds with deposition of bioactive hydroxyapatite and collagen using ice-based microporogens. *Acta Biomater*. 2010;6(6):2013-2019.
- [28] Möllers S, Heschel I, Damink LH, et al. Cytocompatibility of a novel, longitudinally microstructured collagen scaffold intended for nerve tissue repair. *Tissue Eng Part A*. 2009;15(3):461-472.

(Edited by Zhang Y, Zhao H/Yang Y/Song LP)